THERMAL ACTIVITY EXPLORATION AND MONITORING OF RECENTLY ACTIVE KIRISHIMA VOLCANO IN THE SOUTHERN KYUSHU ISLAND IN JAPAN USING SATELLITE IMAGERIES

Md. Bodruddoza Mia[1, 2*], Jun Nishijima[1] and Yasuhiro Fujimitsu[1]
[1]Department of Earth Resources Engineering, Faculty of Engineering, Kyushu University, Fukuoka 819-0395, Japan
[2]Department of Geology, Faculty of Earth and Environmental Science, University of Dhaka, Dhaka-1000, Bangladesh
Corresponding Author's E-mail: bodruddoza@mine.kyushu-u.ac.jp

Keywords: *satellite image, hydrothermal alteration, land surface temperature, radiative heat loss, heat Discharge rate, kirishima volcano.*

ABSTRACT

Recently, a Plinian or sub-plinian eruption occurred from January – September 2011 after a long dormant period in the Kirishima volcano at southern Kyushu Island in Japan. Our purpose is to apply satellite images to explore and monitor the recent thermal activity of this volcano. We used a recent Landsat 8 OLI image for exploring the thermal ground using various hydrothermal alteration mapping techniques and three ASTER thermal infrared images for exploration and monitoring heat losses from this volcano before and after the 2011 eruption. Firstly, the most active region was explored using the alteration mapping techniques such as band combination, band ratio and principal component analysis. For heat loss studies, we selected a target area of about 120 sq. km and used the Stefan-Boltzmann equation to derive the radiative heat flux (RHF), NDVI threshold method for emissivity and Split-window algorithm for land surface temperature (LST). Finally, total radiative heat loss (RHL) was multiplied using a relationship coefficient to estimate and monitor the total heat discharge rates (HDR) from this volcano. The result showed that the highest maximum apparent LSTs above ambient were estimated to be about 9°C, 35°C and 6°C respectively in 2009, 2012 and 2015. The maximum RHFs were calculated apparently about 42 W/m^2, 177 W/m^2 and 29 W/m^2 respectively in the year of 2009, 2011 and 2015. Total HDRs were estimated to be about 9294 MW, 60565 MW and 3160 MW respectively in 2009, 2012 and 2015 after multiplying the total RHL of the respective years of the study using the relationship coefficient. The monitoring shows that the thermal activity or heat loss increased sharply by the eruption and decreased after eruption in this active volcano. The study inferred that the applied methods could be used with an effective and efficient way for monitoring the future thermal status of this active volcano using satellite images.

1. INTRODUCTION

The study area, Kirishima volcano is situated in the southern Kyushu island of Japan, consist of more than 20 basaltic-andesite volcanoes (Kato and Yamasato, 2013) (Fig. 1). It has a number of active craters in this group of volcano of which, Shinmoedake began a series of eruptions on January 19, 2011 (Miyabuchi et al., 2013). Firstly, a small phreatomagmatic eruptions occurred and then it shifted to magmatic eruption on January 26, categorised as a subplinian eruptions (Miyabuchi et al., 2013). Successively, lava filled up the crater up to February 9, 2011 and the eruption activity in this volcano declined. According to Miyabuchi et al. (2013), the largest vulcanian explosions occurred on March 13, 2011, followed by a small eruptions happened up to September 7, 2011. Before eruption in 2011, this volcano was inflated by the magma supply and experienced a repeated phreatic eruption during 2008 to 2010 (Kato and Yamasato, 2013; Miyabuchi et al., 2013) and that might cause the higher heat loss of this volcano but no research on the heat loss from this volcano has done using satellite thermal infrared data yet. Satellite images are used nowadays for a variety of study in the volcanic areas such as for hydrothermal alteration mapping, lava flows course, radiative heat flux and heat discharge studies etc. (Mia and Fujimitsu, 2012; Mia et al., 2012; Mia et al., 2013). Our intention is to apply the Landsat 8 OLI/TIRS satellite image the first time to explore the thermally active region of the Kirishima volcano using alteration mapping and then to estimate and monitor the heat loss from the most active region by the time of recent eruption in 2011 and afterward using three sets of available and good quality ASTER satellite images.

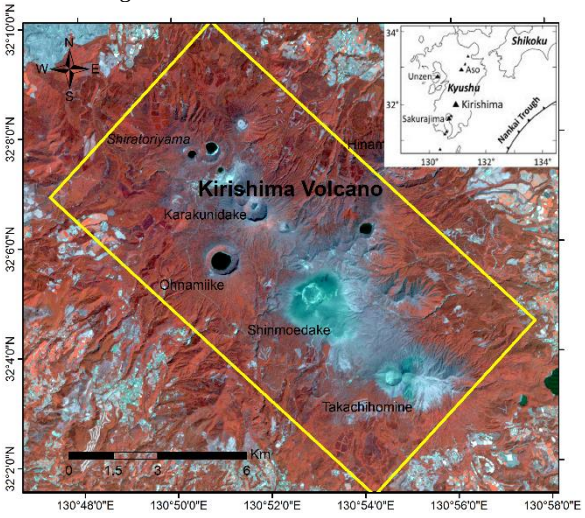

Figure 1: Location map of the study. Heat loss study area shows as yellow box about 120 sq.km.

2. GEOLOGICAL SETTINGS

Kirishima is a cluster of more than 25 andesitic stratovolcanoes with distinct two calderas of quaternary age (Imura and Kobayashi, 2001). It spans about 25 km from north to south and 30 km from east to west (Miyabuchi et al., 2013). This composite volcano is divided into two groups such as older Kirishima and younger Kirishima volcanoes (Imura and Kobayashi, 2001; Miyabuchi et al., 2013). The characteristics of older Kirishima volcano involves two large pyroclastics flows such as Kobayashi–Kasamori and Kakuto pyroclastic flows, formed from 600 ka to 330 ka, and these

volcanic products are exposed now only in the western foot of the Kirishima volcano (Imura and Kobayashi, 2001). The younger Kirishima volcano started to form at 330 ka by the series of eruptions of plinian, vulcanian, strombolian and phreatomagmatic eruptions, which produced numerous fallout tephra layers and gave rise to more than 25 small stratovolcanoes and pyroclastic cones, including Kurinodake Volcano (200–100 ka), Ebinodake (100–50 ka), Onamiike (45 ka), Ohatayama (45–38 ka), Hinamoridake (38 ka), Futagoishi (38–30 ka), Iimoriyama (29–22 ka), Karakunidake (the highest peak of Kirishima Volcano; 22–15 ka), Koshikidake, Shinmoedake (10.4 ka-present), Takachihonomine (8.1–6.8 ka), Miike maar (4.6 ka) and Ohachi (8–18C) (Nagaoka and Okuno, 2011)

3. MATERIALS AND METHODS

We used two different sensor's satellite images in this study, one is Landsat 8 OLI/TIRS, used for exploring the thermal ground and the other one is ASTER that used for exploration and monitoring heat losses from the most active part of Kirishima volcano before and after the recent 2011 eruption. The Landsat 8 image was acquired on February 19, 2017 and that was used for identifying various hydrothermal indicator minerals using various conventional techniques of altered minerals mapping such as band combination, band ratio, and principal component analysis for exploration of the most active thermal ground in this volcano. After delineating the most active part of the Kirishima volcano, we used night time ASTER thermal band data for monitoring land surface temperature and radiative heat loss, and day time ASTER images for emissivity estimation from the study area. The ASTER images were acquired on 12 May 2009 (day), 6 April 2009 (night), 29 January 2012 (day), 13 March 2012 (night) and 26 March 2015 (day), 5 May 2015 considering good quality and availability in this study area. Meteorological data such as ambient temperature, relative humidity were collected from the Miyazaki Miyakonojo met station (154 m above mean sea level) of AMEDAS and later on, these data were adjusted with altitude variation between the station and Shinmoedake (1420 m above mean sea level) at Kirishima volcano using the international standard atmosphere (ISA) method (Talay, 1975; Airbus, 2000).

The hydrothermal alteration techniques are colour composites (or band combination 7:3:5 and 7:5:3), band ratio such as Abram, Chica-Olma, Kaufmann ratio, principal component analysis and Crosta techniques (Mia and Fujimitsu, 2012). The Day time ASTER images were used to calculate emissivity based on NDVI value for each land-covers and the night time thermal infrared (TIR) bands were used for land surface temperature calculation for heat flux estimation and monitoring within the study area. The night time images were selected to avoid the solar effect in this study. The NDVI threshold method was applied for the emissivity measurement of this study (Qin et al., 2006). Then, the thermal band data were used to convert into radiance value from DN of the selected night time satellite images of this study using the metadata of those images with necessary equation (Qin et al., 2006). The radiance value was used to calculate brightness temperature of the study area at sensor's information without considering the atmospheric effects. This brightness temperature was used to estimate true skin temperature of the ground of this study using split-window algorithm with the TIR band 13 and band 14 (Qin et al., 2001; Qin et al., 2006). Later on, the radiative heat flux was calculated using the Stefan-Boltzmann equation in this study from 2009 to 2015 within the most active Kirishima volcanic area (Mia et al., 2012; Mia et al., 2014). We used a relationship coefficient (6.49 or about 15%) between radiative heat flux and heat discharge rate to calculate the total heat loss and monitor the trend of heat discharge rate in this study area (Mia et al., 2013).

4. RESULTS AND DISCUSSION

The colour composite method used three additive colours (i.e., red, green, blue or RGB) to display multispectral bands of Landsat 8 image where the spectral response of land covers such as vegetation, water, rock or minerals indicating maximum in their reflectance. The band combination of 7:3:5 showed in RGB as blue for vegetated, and brighter green-red for altered clay minerals or hydrothermal altered zone showing as most active in the Kirishima volcano (Fig.2A). Another band combination 7:5:3 showed in RGB as green for vegetated and brighter reddish-blue region indicates altered region or most active volcanic zone (Figure 2B). From the band ratio analysis, the hydrothermal altered region showed as light green, deep green and reddish cyan respectively in Abram, Chica-Olma and Kaufmann ratio analysis indicating the most active regions in the Kirishima volcano (Fig. 2 C, D, E). The principal component analysis (PCA) is a principal component transformation (PCT) technique to reduce the dimensionality of correlated multispectral data. This analysis was applied on six Landsat OLI bands of the study area (Table 1). The PCT of unstretched bands 2, 5, 6, 7 is used to detect clay minerals, where PC4 corresponds to a 'hydroxyl image' or H image (Aguilera et al., 2016) (Table 1). The figure 2F shows the hydroxyl minerals as bright pixel around the craters of the Kirishima volcano. The PCT for bands 2, 4, 5, and 6 is used to detect iron oxide minerals, where the PC4 corresponds to an 'iron oxide image' or F image (Aguilera et al., 2016) (Table 1). The figure 2G shows iron oxide minerals concentrated as around the craters of this volcano shown as bright pixel. In case of Crosta techniques, the information stored on the hydroxyl (H) and iron-oxide (F) images was used to combine producing a map displaying the pixels with anomalous concentrations of both iron-oxide and hydroxyl type of minerals as bright (Mia et al., 2012). So, by applying the Crosta images of H: H+F: F in RGB combinations displayed a dark bluish colour composite image where the alteration regions are shown as bright pixels around the craters of the Kirishima volcano (Fig. 2H).

Table 1: Principal component analysis

Principal Component Analysis for six bands

Eigenvector	Band 2	Band 3	Band 4	Band 5	Band 6	Band 7	Eigenvalue (%)
PC1	0.131	0.187	0.265	0.495	0.658	0.446	68.186
PC2	-0.094	-0.099	-0.215	0.856	-0.262	-0.366	28.901
PC3	0.466	0.509	0.576	0.060	-0.399	-0.171	2.584
PC4	0.036	-0.024	-0.175	0.125	-0.564	0.796	0.222
PC5	0.679	0.241	-0.674	-0.048	0.145	-0.061	0.087
PC6	0.543	-0.798	0.258	0.029	-0.007	-0.001	0.021

Principal Component Analysis of bands 2,5,6,7

Eigenvector	Band 2	Band 5	Band 6	Band 7	Eigenvalue (%)
PC1	0.126	0.573	0.676	0.445	68.637
PC2	-0.106	0.808	-0.373	-0.444	30.219
PC3	0.945	0.052	-0.300	0.121	0.915
PC4	-0.283	0.127	-0.560	0.768	0.229

Principal Component Analysis of bands 2,4,5,6

Eigenvector	Band 2	Band 4	Band 5	Band 6	Eigenvalue (%)
PC1	0.123	0.245	0.697	0.662	68.941
PC2	-0.162	-0.356	0.710	-0.586	28.613
PC3	-0.551	-0.691	-0.094	0.458	2.342
PC4	-0.809	0.579	0.028	-0.094	0.104

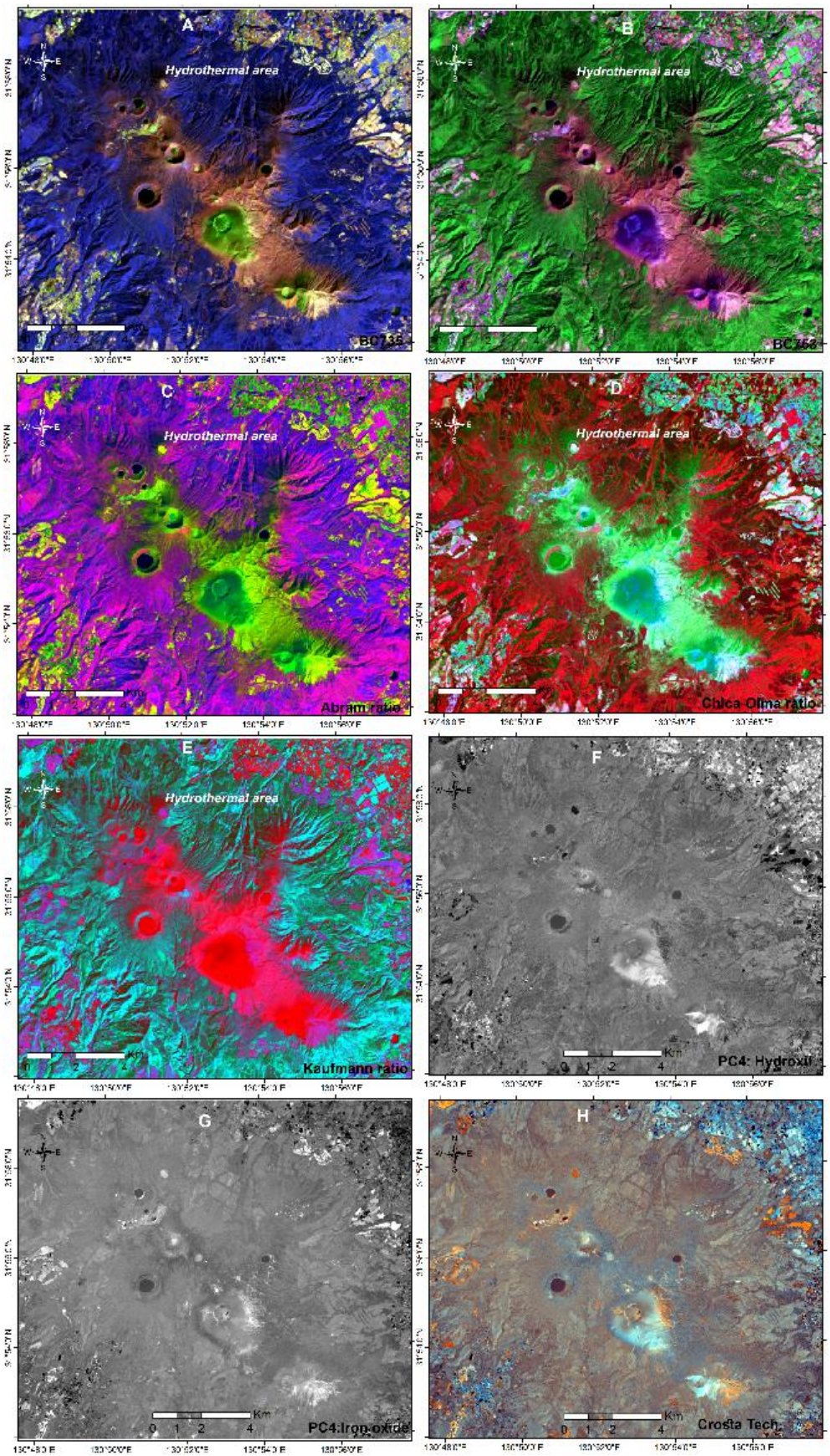

Figure 2: Hydrothermal alteration mapping of the Kirishima volcano: Band combination results shown in figure A &B; Band ratio results in the figure C, D &E; Results of PCA in the figure F, G and H.

From the hydrothermal alteration mapping, we selected the most active region of thermal activity about 120 sq. km area of the Kirishima volcano for heat loss exploration and monitoring by the time of recent eruption and afterward using ASTER thermal infrared data (Fig.1). We used the ASTER daytime image to derive the emissivity of the landcover of the study area using the NDVI value of each year image respectively in 2009, 2012 and 2015. We obtained the emissivity value in the ranges of 0.96 to 0.99. Later on, we used the NDVI value to divide the land covers into four types such as water/wetland (NDVI<0), bared (NDVI= 0-0.2), mixed (NDVI= 0.2-0.5) and vegetated land (NDVI>0.5) (Fig. 3). We obtained the area of water or wetland increased sharply up to 70 sq. km from 2009 to 2012 by the eruption time and then declined to 0.39 sq. km of the total study area in 2015 (Table 2). Bared and mixed land declined as water/wet land increased by the time of eruption from 2009 to 2012 and there was no healthy vegetated region actually as the vegetated region covered by ash. After the eruption, we obtained a huge land of mixed and healthy vegetation in 2015 respectively about 90 sq. km and 23 sq. km (Fig.3). The maximum apparent land surface temperature above ambient increased sharply from about 9°C to 35°C by the eruption period from 2009 to 2012 and then declined rapidly in the year of 2015 about 6°C (Fig.4; Table 2). The radiative heat flux (RHF) also increased apparently from 2009 to 2012 by the eruption period with coinciding LST of this volcanic area. The maximum apparent RHF was about 42 W/m^2 in 2009 and then increased sharply to about 177 W/m^2 in 2012 then declined to about 29 W/m^2 in 2015 (Fig. 5; Table 2). Total radiative heat losses of this study area were apparently about 1439 MW, 9375 MW, and 489 MW respectively in the year of 2009, 2012 and 2015 (Table 2). After multiplying the total RHL using a relationship coefficient between RHF and HDR (i.e., 6.49), we obtained the total HDR about 9294 MW, 60565 MW and 3160 MW respectively in 2009, 2012, and 2015 (Fig. 6; Table 2). In discussion, the study showed extreme behavior of thermal activity during or by the time of eruption from 2009 to 2012 and then decline of the thermal activity afterward up to 2015 in the Kirishima volcanic zone in all aspect of LST, RFH, RHL and HDR. The eruption activity changes the land cover types during the study period. Satellite images, especially ASTER thermal infrared data, showed efficiently the thermal activity of the recently active volcano in Japan.

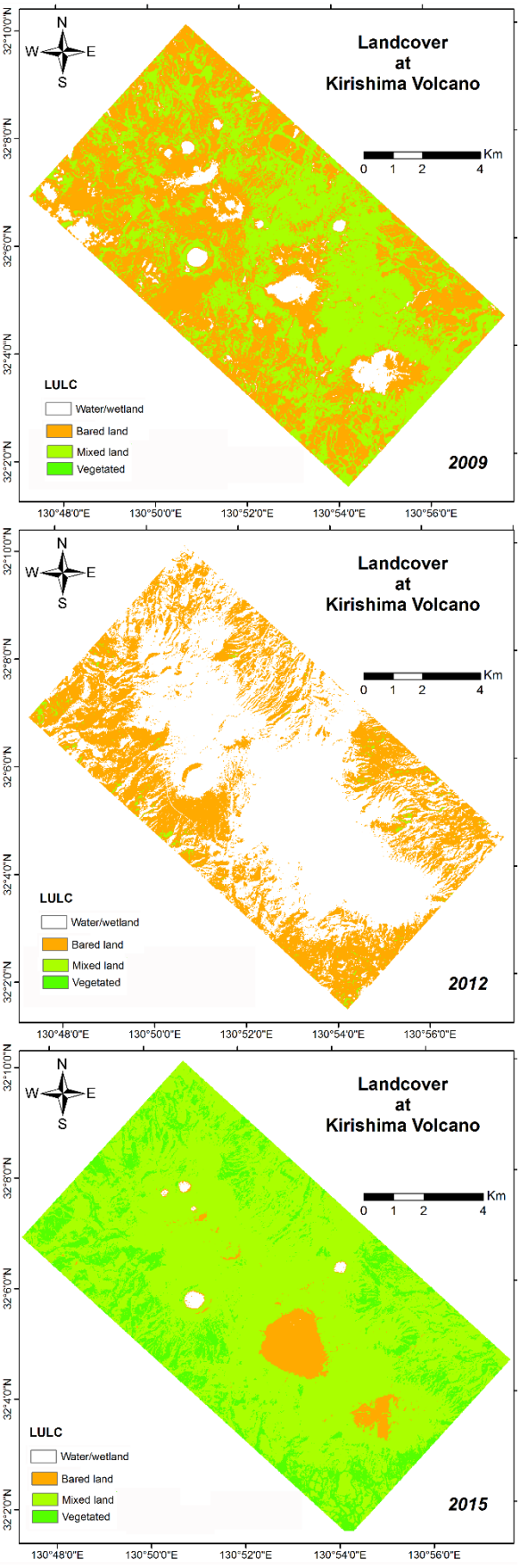

Figure 3: Landuse-landcover (LULC) map of the study area (a yellow rectangle in Figure 1) from 2009 to 2015.

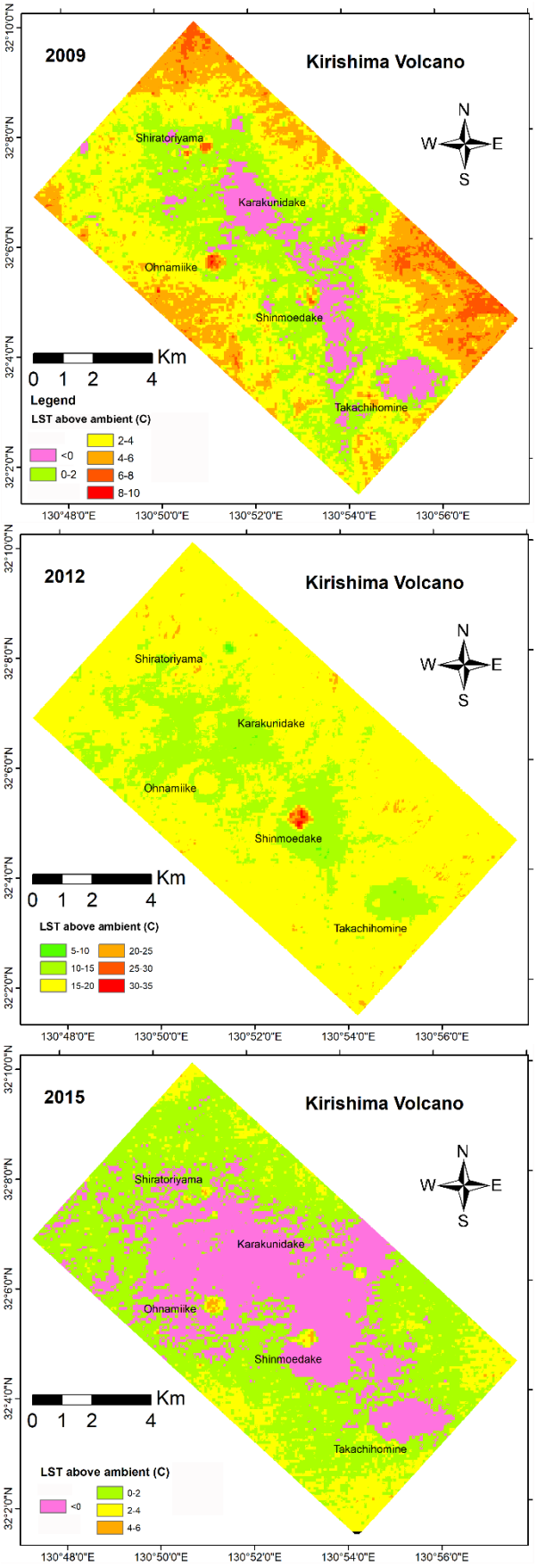

Figure 4: LST above ambient of the study area.

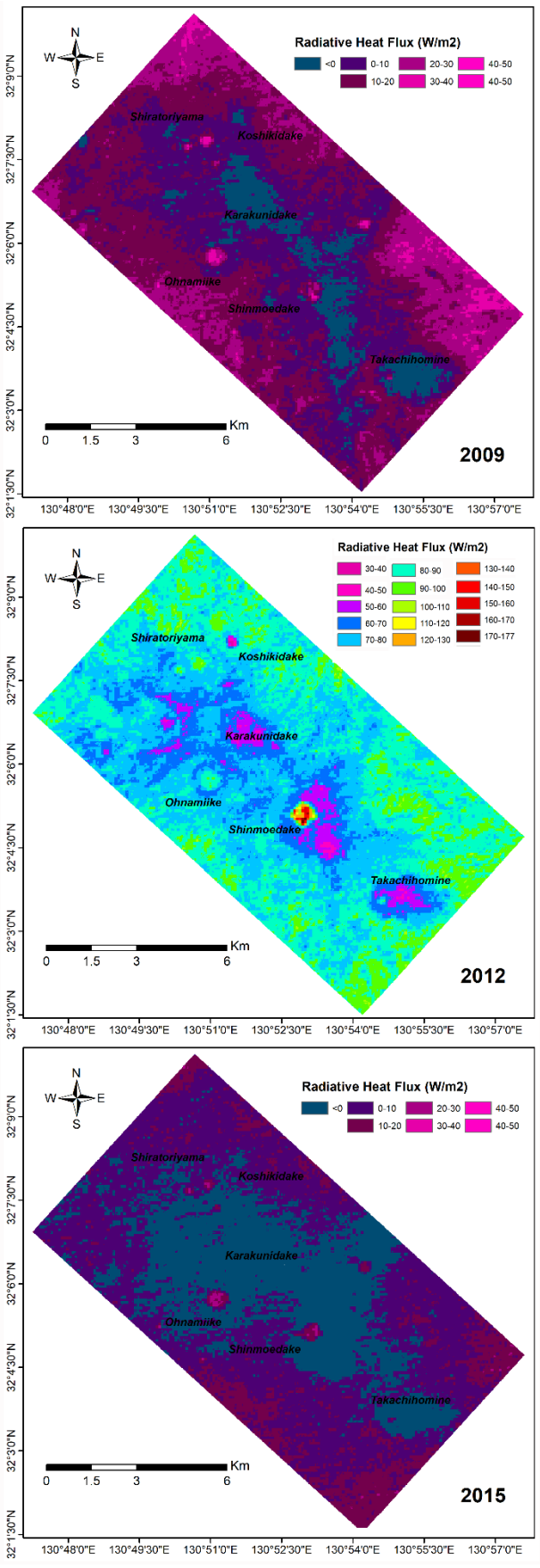

Figure 5: Radiative heat flux of the study area in 2009, 2012 and 2015.

Table 2: Summary results of the study.

Year	Atm. Transmissivity		Ambient Temp. (°C)	LULC (Sq. km)				LST above ambient(°C)		RHF (W/m²)		Total RHL (MW)	Total HDR (MW)
	B13	B14		Water	Bared	Mixed	Vegetated	Min	Max	Min	Max		
2009	0.89	0.83	9.77	6.48	58.99	53.10	0.00	-4.56	8.64	-20.67	41.82	1438.63	9293.55
2012	0.95	0.92	-3.63	69.97	43.96	1.02	0.00	0	35.06	0.00	177.08	9375.38	60564.95
2015	0.93	0.89	2.57	0.36	5.31	89.78	23.19	-4.61	5.69	-22.65	28.98	489.24	3160.49

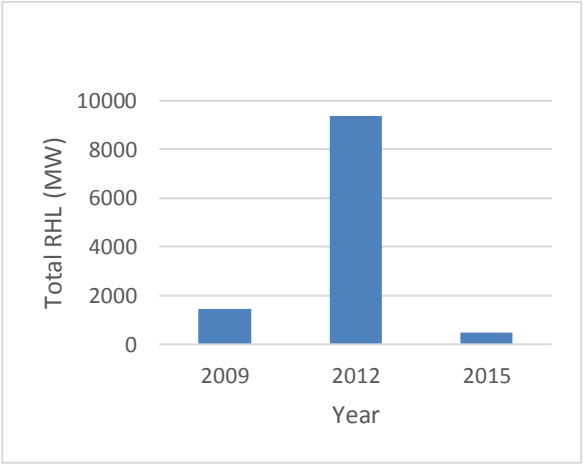

Figure 6: Results of the total heat loss of the study area before and after the eruption of the Kirishima volcano in 2011.

5. CONCLUSION

Satellite images used successfully to explore and monitor the recent thermal activity of the Kirishima volcano. Landsat 8 OLI image showed efficiency for exploring the thermal ground using various hydrothermal alteration mapping techniques such as band combination, band ratio and principal component analysis. ASTER thermal infrared data was used to explore and monitor heat loss from the volcano by the time of eruption and afterward. We obtained the highest maximum apparent LST above ambient in 2012 about 35℃ by the time of recent eruption in 2011 in this volcano, and the lowest maximum LST above ambient was in 2015 about 6℃. The maximum RHFs were estimated apparently about 42 W/m^2, 177 W/m^2 and 29 W/m^2 respectively in the year of 2009, 2011 and 2015. Total heat losses were estimated to be about 9294 MW, 60565 MW and 3160 MW respectively in 2009, 2012 and 2015. The study shows that the thermal activity or heat loss increased sharply by the eruption and decreased after eruption in this active volcano. The study concluded that the Landsat and ASTER images could be used with an effective and efficient way for exploration and monitoring the future thermal status of this active volcano.

ACKNOWLEDGEMENTS

We acknowledge the Grant-in-Aid for JSPS fellow's research fund supported for this research. The first author is an overseas researcher under Postdoctoral Fellowship of Japan Society for the Promotion of Science (P16081). The authors gratefully thank the Editor and reviewers for upgrading the manuscript. We also acknowledge the USGS archives authority to support the satellite imageries for this research with free of cost. Special thanks to the authority of Japan Meteorological Agency to provide the necessary weather data for this research.

REFERENCES

Aguilera, F., Layana, S., Rodriguez-Diaz, A., Gonzalez, C., Cortes, J. and Inostroza, M.: Hydrothermal Alteration, Fumarolic Deposits and Fluids from Lastarria Volcanic Complex: A multidisciplinary study. *Andean Geology*, vol. 42, pp. 166-196, (2016).

Airbus: Getting to Grips with Aircraft Performance, *Airbus Indusrie, Customer Services*, Blagnac, pp. 11-16, (2000).

Kato, K. and Yamasato H.: The 2011 eruptive activity of Shinmoedake volcano, Kirishimayama, Kyushu, Japan—Overview of activity and Volcanic Alert Level of the Japan Meteorological Agency—. *Earth Planets Space*, vol. 65, pp. 489-504, (2013).

Imura, R.and Kobayashi, T.: Geological map of Kirishima Volcano (1:50,000). Geological Map of Volcanoes 11, *Geological Survey of Japan* (in Japanese with English abstract). (2001).

Mia, M.B., Bromley, C.J., Fujimitsu Y.: Monitoring heat flux using Landsat TM/ETM + thermal infrared data-A case study at Karapiti ('Crater of the Moon') thermal area, New Zealand. *Journal of Volcanology and Geothermal Research*, vol. 235-236, pp.1–10, (2012).

Mia, M.B. and Fujimitsu, Y.: Mapping hydrothermal altered deposits using Landsat 7 ETM + image in and around Kuju volcano, Kyushu, Japan. *Journal of Earth System Sciences*, vol. 121 (4), pp.1049–1057, (2012).

Mia, M.B., Bromley, C. J., Fujimitsu Y.: Monitoring heat losses using Landsat ETM + thermal infrared data: a case study in Unzen geothermal field, Kyushu, Japan. *Pure and Applied Geophysics*, vol. 170 (12), 2263–2271, (2013).

Mia, M.B., Nishijima, J., Fujimitsu, Y.: Exploration and monitoring geothermal activity using Landsat ETM + images-A case study at Aso volcanic area in Japan. Journal of Volcanology and Geothermal Research, vol. 275, pp.14-21, (2014).

Miyabuchi, Y., Hanada, D., Niimi, H., Kobayashi, T.: Stratigraphy, grain-size and component characteristics of the 2011 Shinmoedake eruption deposits, Kirishima Volcano, Japan. *Journal of Volcanology and Geothermal Research*, vol. 258, pp. 31-46, (2013).

Nagaoka, S.and Okuno, M.: Tephrochronology and eruptive history of Kirishima volcano in southern Japan. *Quaternary International*, vol. 246, pp. 260–269, (2011).

Talay, T.A.: Introduction to the aerodynamics of flight, NASA SP -367, *National Aeronautics and Space Adminstration*, Washington, D.C., pp. 6-9, (1975).

Qin, Z., Karnieli, A., Berliner, P.: A mono-window algorithm for retrieving land surface temperature fromLandsat TM data and its application to the Israel–Egypt border region. Int. J. Remote Sens. Vol. 22 (18), pp. 3719–3746. (2001).

Qin, Z., Li, W., Gao, M., Zhang, H.: An algorithm to retrieve land surface temperature from ASTER thermal band data for agricultural drought monitoring. *Proceeding of SPIE*, vol. 6359, pp. 63591F1-F8, (2006).